Check for updates

Macromolecular Chemistry and Physics
www.mcp-journal.de

Polymers Diffusivity Encoded by Stimuli-Induced Phase Transition: Theory and Application to Poly(*N*-Isopropylacrylamide) with Hydrophilic and Hydrophobic End Groups

Sjören Schweizerhof, Dan Eugen Demco, Ahmed Mourran,* Radu Fechete, and Martin Möller**

The self-diffusion of various nano-objects investigated by high-resolution nuclear magnetic resonance diffusometry proves to be an efficient method for the characterization of dynamics, aggregation kinetic, and matrix morphology. This study investigates how the two-state model and Boltzmann function approach can be used for the evaluation of the thermodynamic parameters of temperature-induced phase transition encoded in polymer diffusivity. The characteristics of the phase transition given by the transition temperature, change of entropy, and width of transition are obtained for poly(*N*-isopropylacrylamide) (PNIPAm) linear polymers with hydrophilic and hydrophobic end-group functionalization. The effect of end groups upon the polymer diffusivity is investigated as a function of molecular weight (M_n), from which fractal dimensions and hydrodynamic drag coefficients are obtained. The PNIPAm diffusivity is affected strongly by the end groups, and it is reflected in the hydrodynamic radius dependence upon molecular weight that obeys different power-law relations. In this study, the synthesis of α-ω-heterotelechelic PNIPAm of different molecular weights with a thiol end group and a hydrophilic NIPAm-like as well as a hydrophobic benzyl end group are described by reversible addition–fragmentation chain-transfer polymerization.

1. Introduction

Translational motion of molecules, nanoparticles, and proteins in solutions plays a central role in modern science.[1–3] The correlation between diffusion and chemical and biological phenomena is of particular importance. This molecular process not only reflects intrinsic properties of the diffusing species itself, but can also shed light on the surrounding environment.[4–6] Stochastic mass transport measurements of water in polymers, microgels, gels, proteins, proton-exchange membranes, porous materials, and brain by noninvasive nuclear magnetic resonance (NMR) methods proved to be an accurate technique for evaluation of diffusivity tensor D as well as its dependence of the surrounding morphology and architecture.[1–11]

Dynamic light scattering (DLS) technique gives access to the diffusion coefficients of polymers and microparticles with low concentration into solvent. The decay of electrical field autocorrelation function can be analyzed by the sum of two exponential decays that depend on translation and rotation diffusion coefficients of centrosymetric particles.[12,13] Fluorescence correlation spectroscopy uses fluorophores attached to the diffusing molecule, macromolecules, or proteins possessing a large temporal linear dynamic range allowing single-molecule sensitivity.[14,15] A noninvasive method is represented by NMR diffusometry applied to the polymers and proteins in solutions that are sensitive to the molecular weight,[16–21] shape of the molecules,[21,22] fractal dimension,[16–21] and the aggregation state, as discussed in ref. [3], and references therein. A power law describes the dependence of the isotropic diffusivity D upon the molecular weight M_n for as given homogeneous family of molecules, i.e., $D \propto 1/(M_n)^{1/d_F}$, where d_F is the fractal dimension.[21] This

S. Schweizerhof, Prof. D. E. Demco, Dr. A. Mourran, Prof. M. Möller
DWI-Leibniz-Institute for Interactive Materials, e.V.
RWTH-Aachen University
Forckenbeckstraße 50, D-52074 Aachen, Germany
E-mail: demco@dwi.rwth-aachen.de; mourran@dwi.rwth-aachen.de; moeller@dwi.rwth-aachen.de

The ORCID identification number(s) for the author(s) of this article can be found under https://doi.org/10.1002/macp.201700587.

© 2018 The Authors. Published by WILEY-VCH Verlag GmbH & Co. KGaA, Weinheim. This is an open access article under the terms of the Creative Commons Attribution License, which permits use, distribution and reproduction in any medium, provided the original work is properly cited.

The copyright line for this article was changed on 3 July 2020 after original online publication.

DOI: 10.1002/macp.201700587

Prof. D. E. Demco, Prof. R. Fechete
Department of Physics and Chemistry
Technical University of Cluj-Napoca
25 G. Baritiu Str., RO-400027 Cluj-Napoca, Romania

Prof. M. Möller
Institute of Technical and Macromolecular Chemistry
RWTH-Aachen University
Worringerweg 2, D-52074 Aachen, Germany

© 2018 The Authors. Published by WILEY-VCH Verlag GmbH & Co. KGaA, Weinheim

relationship was proved to be valid for small molecules and linear homopolymers but it is an approximation for polymer rods. Moreover, the dependence of the diffusivity on the molecular weight and fractal dimension can be used for evaluating M_n for a given class of molecules.[21] Furthermore, we should note that such an investigation was not made for poly(*N*-isopropylacrylamide) (hereafter, PNIPAm) with different end-group functionalization in aqueous solution.

Understanding polymer diffusivity in the presence of stimuli-induced phase transition is of importance for design of drug delivery carriers and for controlled multidimensional assembly that can be achieved by functionalizing nanoparticles with polymer brushes. For the last purpose, gold nanorods (AuNRs) are such nanoparticles with unique electrical and optical properties having strong surface plasmon resonances in the visible range.[23] Furthermore, stimuli-responsive polymers tethered on the gold nanoparticles will open new possibilities for temperature-controlled nanoheater applications induced by near-infrared irradiation.[24–26] To this point, soft microrobots employing non-equilibrium actuation via plasmonic heating were developed.[27]

Self-diffusion can be investigated chemically selective using high-resolution NMR diffusometry that differentiates between the stochastic mass transport of polymers and solvent.[1–3] The diffusivity was measured for swollen and collapsed states of PNIPAm microgels using the pulsed-field-gradient spin-echo NMR (PFGSE-NMR) method applied to the methyl side-chain NMR resonance but no thermodynamic parameters related to this process were reported.[28] Furthermore, concentration and temperature dependences of coil-to-globule transition of PNIPAm graft copolymers were investigated by polymer diffusion studies.[29] The PFGSE-NMR method was used to measure diffusion coefficient of the star and linear PNIPAm as a function of temperature for different molecular weights.[30] Another microscopic indicative for volume phase transition was shown to be solvent diffusivity in aqueous dispersion of PNIPAm microgels.[31] Moreover, coil-to-globule collapse and intermolecular aggregation of nonfunctionalized PNIPAm in aqueous solution upon exceeding the lower critical solution temperature (LCST) was investigated by NMR diffusometry under a temperature-jump condition.[32]

Besides polymer and solvent diffusivity studies, an independent access to phase-transition thermodynamic parameters is given by the measurement of changes in the polymer conformations reflected in ^{1}H high-resolution magic-angle sample spinning (HRMAS) NMR spectroscopy edited by transverse magnetization relaxation (T_2) via integral peak intensity. This approach was applied to investigate thermodynamic parameters in the process of temperature-induced phase transition and applied to the stimuli-responsive PNIPAm linear polymers and brushes onto AuNRs.[33,34] The dependences on the molecular weight and end-group functionalization were reported for the transition temperature, transition entropy, and width of temperature-induced transition.[33,34] The molecular process behind this NMR method is related to the polymer side chains and segmental dynamics changes that occur in the hydrophilic-to-hydrophobic transition, which affects transverse magnetization relaxation and, hence, the spectral line width.[33–36]

The aim of this study is to investigate with a two-state model the interplay between the temperature-induced phase transition of stimuli-responsive polymer brushes based on linear PNIPAm in aqueous solutions and its diffusivity. It is shown that thermodynamic quantities of the phase transition can be measured from the self-diffusing coefficients of the involved species. This study is focused on the dependences of PNIPAm's apparent diffusivity upon temperature, molecular weight, and end-group functionalization. The fractal dimension, transition temperature, transition entropy, width of transition, and hydrodynamic radius were evaluated for PNIPAm linear polymers functionalized with a hydrophilic and a hydrophobic end group using ^{1}H NMR diffusiometry and compared to the information obtained from DLS.

2. Experimental Section

2.1. Sample Preparation

The materials used for preparation of linear PNIPAm with different molecular weights and end-group functionalization in aqueous solution were reported in the previous publications.[33,34] The synthesis and characterization of polymer by size exclusion chromatograph (SEC), UV–vis spectrophotometry (UV-Vis), transmission electron microscopy (TEM), gas liquid chromatography-mass spectrometry (GC-MS), differential scanning calorimetry (DSC), and NMR spectroscopy of hydrophobic end-group functionalized PNIPAm with benzyl and thiol (hereafter, Bn-PNIPAm-SH) were described before in details.[33] The same steps in synthesis were used for the preparation of hydrophilic PNIPAm end-group functionalized with an NIPAm-like and thiol end group (hereafter, NIPAm-PNIPAm-SH).[34] Additional information is reported in the Supporting Information.

2.2. Proton HRMAS NMR Spectroscopy

Proton HRMAS NMR spectral measurements were made on a wide bore AV700 Bruker NMR spectrometer operating at frequency of 700.2378 MHz, equipped with a cross-polarization MAS probe with a 3.2 mm rotor. The rotor frequency was set at 5 kHz. The temperature was changed in the range from 10 to 70 °C and was maintained within ± 0.5 K using a Bruker temperature control unit. All the ^{1}H HRMAS spectra were externally referenced to tetramethylsilane (TMS). For all measurements, the recycle delay was 7 s, the radio-frequency pulse length was 1.9 µs, while the dwell time was 10 µs, and the number of scans was 64. The time domain data were 4k and the zero filling was done with 16k.

2.3. Proton Pulsed-Field-Gradient-Stimulated Echo NMR Diffusometry

The apparent diffusivity D of linear PNIPAm end-group functionalized with benzyl and NIPAm was measured using an AV700 Bruker NMR wide bore spectrometer with a Diff50 Bruker unit and by pulsed-field-gradient stimulated echo (PFGSE) sequence of Stejskal and Tanner.[37] The experiment

© 2018 The Authors. Published by WILEY-VCH Verlag GmbH & Co. KGaA, Weinheim

is 2D, by recording the dependence of the NMR peak integral intensity upon the applied field gradient strength. The apparent diffusivity was obtained by fitting the normalized stimulated spin-echo decay as a function of gradient strength g to the Stejskal–Tanner equation[37]

$$\frac{I(g)}{I_0} = \exp\left\{-qD\left(\Delta - \frac{\delta}{3}\right)\right\} \quad (1)$$

where the convention $q = \gamma\delta g$ is employed for the diffusion wave vector.[1–3] In Equation (1), $I(g)$ is the integral intensity of the methyl peak or aliphatic spectral region obtained by the Fourier transform of the half-decay of stimulated echo at a given value of magnetic field gradient g, and I_0 is the integral intensity for small values of field gradient value compared to the maximum of the gradient strength g_{max}. Equation (1) can be rewritten as

$$\frac{I(g)}{I_0} = \exp\{-bD\} \quad (2)$$

where the quantity b is defined as $b = \gamma^2 g^2 \delta^2 \left(\Delta - \frac{\delta}{3}\right)$. The magnetogyric ratio is denoted by γ, δ is the duration of the gradient pulse, and Δ is the diffusion time defined as the time interval between the gradient pulses. In all the ^{1}H high-resolution NMR diffusometry experiments reported in this study, the delays were set to $\delta = 2$ ms and $\Delta = 20$ ms. A field gradient g in the z-direction was applied, increased in 16 steps in a linear ramp from 2% to 95% of maximum field gradient in the range of $g_{max} = (1 \div 10)$ T/m. The stimulated echo decay was collected into 16k data points and Fourier transformed by applying zero-filling to 32k data points and an exponential window function with a line broadening factor of 5 Hz. A relaxation delay of 7 s was used with a spectral window of 6 kHz. For all NMR measurements made in deuterated aqueous solutions, the PNIPAm concentration was of 50 mg mL^{-1}. For both CPMAS 3.2 and Diff 50 NMR probeheads, the temperature calibration was made using neat ethylene glycol chemical shift resonances. The intensity of the NMR free-induction decay and, hence, the detected normalized stimulated echo is proportional to the Curie factor and, hence, depends on the inverse of temperature. In the following, this dependence would be neglected in the limited range of temperatures 10–60 °C used in these NMR measurements. The sample temperature was controlled by a gradient cooling system to avoid convection effects induced by small temperature gradient in the radio-frequency insert.

3. Theory

3.1. Temperature-Induced Phase Transition by a Two-State Model Applied to Diffusometry

The self-diffusion temperature dependence of a responsive polymer at different time scales can be associated with the following processes: i) coil-to-globule transition that can lead to the change in the individual polymer size and conformations, ii) aggregation that changes the size and shape of the particles, and iii) colloids' precipitation. For the concentration c of the polymer in solution well above the overlap threshold concentration c^* ($c > c^*$), formation of intermolecular aggregation has taken place.[17,38] Furthermore, it was reported that for intermediate concentration in the semidilute regime[17] of PNIPAm in aqueous solution yields colloidal stable dispersion above LCST.[39–42] In this case, at temperature above LCST, the effect of stimuli-induced phase transition revealed by diffusivity could compete with the aggregation process. The NMR spectroscopy and relaxometry that edits the temperature-induced phase transition in responsive NIPAm-PNIPAm-SH and Bn-PNIPAm-SH polymers in D_2O with a concentration of $c = 50$ mg mL^{-1} for low and intermediate values of M_n revel the transition between two well-defined states of coil and globular polymers.[33,34] Hence, we consider that for the used polymer concentration in the overlap regime and in the time window of the experiments, the process of transition is dominated by the thermal responsiveness of the polymers and not by aggregation followed by precipitation. This was shown for PNIPAm with concentrations of $c = 1$–10 mg mL^{-1}.[30]

A quantitative description of the temperature-induced phase transition of responsive linear polymers and brushes was developed based on a two-state model.[33] The main assumptions of the model are reviewed in the following sections. The ensemble of polymer chains, brushes, or microparticles in aqueous solutions is assumed to evolve under constant volume and pressure. The temperature (T) is the only relevant intensive variable. The statistical ensemble is composed of i-subensembles being in pure i-state. In the following, we limit our discussion to the polymer chains in two states (i.e., $i = 1, 2$) represented by, predominately, hydrophilic ($i = 1$, coil state) and hydrophobic ($i = 2$, globule state) polymer chains in thermodynamic equilibrium. This model is similar to that of monomers of the chain that can exist in two distinct and interconverting states.[43–46] The precise identification of the monomeric states leads to the reactive binary[43,46] and ternary systems.[44–46]

For our model,[33] the statistical average of a thermodynamic quantity designed as "observable" $\langle O(T)\rangle$ can be written as

$$\langle O(T)\rangle = \sum_i P_i O_i(T) \quad (3)$$

where $O_i(T)$ is the physical quantity corresponding to each i-state. The probability P_i that the quantity $O(T)$ is in i-state is given by

$$P_i = \frac{\exp(-\beta G_i)}{\sum_i \exp(-\beta G_i)} \quad (4)$$

The Gibbs free energy is $G_i = H_i - TS_i$, where H_i and S_i are the enthalpy and entropy thermodynamic potentials of the i-state, respectively. In Equation (4), $\beta = (k_B T)^{-1}$, where k_B is the Boltzmann constant.

In the case of a statistical ensemble having two states from Equations (3) and (4), we can write in the region of coil-to-globule phase transition as

$$\langle O(T)\rangle = \frac{O_{coil}}{1 + \exp\{-\beta[\Delta H - T\Delta S]\}} + \frac{O_{globule}}{1 + \exp\{\beta[\Delta H - T\Delta S]\}} \quad (5)$$

© 2018 The Authors. Published by WILEY-VCH Verlag GmbH & Co. KGaA, Weinheim

where $\Delta H = H_{globule} - H_{coil}$ and $\Delta S = S_{globule} - S_{coil}$. The statistical quantities O_{coil} and $O_{globule}$ describe the coil and globule polymer chains subensembles in the plateau temperature region around the phase transition. At transition temperature T_t, the state probabilities fulfil the relationship $P_{coil} = P_{globule}$, which implies $\Delta H = T_t \Delta S$. In the narrow temperature region of phase transition, we can write $\beta \approx (k_B T_t)^{-1}$. These assumptions allow us to rewrite Equation (5) as

$$\langle O(T) \rangle \approx \frac{O_{coil}}{1+\exp\left\{\frac{(T_t - T)\Delta S}{k_B T_t}\right\}} + \frac{O_{globule}}{1+\exp\left\{-\frac{(T_t - T)\Delta S}{k_B T_t}\right\}} \quad (6)$$

Equation (6) was derived from first principles of the statistical thermodynamics applied in the region of phase transition. The thermal bath is represented by the hydrogen bonds' network fluctuations of the solvent characterized by temperature T. The interactions between the responsive polymer and solvent are included in phase-transition temperature and change of transition entropy.

In the isotropic large medium the 3D diffusion of polymers can be described by the Einstein relationship[1–3]

$$D = \lim_{t\to\infty} \frac{1}{6t} \langle (\vec{r}\,(t) - \vec{r}\,(0))^2 \rangle \quad (7)$$

where the stochastic position vector $\vec{r}\,(t)$ describes the center-of-mass of the polymer at time t, relative to the origin of coordinate system of reference given by $\vec{r}\,(0)$. The self-diffusion coefficient is denoted by D. The statistical observable is in the case of diffusivity measurements the mean-squared displacement over diffusion time t, i.e., $\langle (\vec{r}\,(t) - \vec{r}\,(0))^2 \rangle$. From Equations (6) and (7) we can write for the temperature dependence of diffusivity.

$$D(T) \approx \frac{D_{coil}}{1+\exp\left\{\frac{(T - T_t)|\Delta S|}{k_B T_t}\right\}} + \frac{D_{globule}}{1+\exp\left\{-\frac{(T - T_t)|\Delta S|}{k_B T_t}\right\}} \quad (8)$$

where T_t and $|\Delta S|/k_B$ are the fit parameters of interest. We assumed that in the plateau temperature regime of coil and globule states, the temperature dependence of diffusivities is weak (see the following sections) and can be described by the average self-diffusion coefficients D_{coil} and $D_{globule}$. In the plateau regimes, the above assumption is partially justified by the weak temperature dependence of hydrodynamic radius and solvent viscosity.

Equation (8) can be used to analyze the two states around the transition temperature of phase transition, i.e., for $T < T_t$ and $T > T_t$, that corresponds to coil or fully hydrated state and globule or collapsed state, respectively. In the swollen state, the temperature difference can be approximated by $T - T_t \approx -T_t$, and from Equation (8), in the limit of $|\Delta S|/k_B \gg 1$, we yield $D \approx D_{coil}$. For collapsed state $T - T_t \approx T$, and we get $D \approx D_{globule}$.

3.2. Temperature-Induced Phase Transition by Diffusometry Described by Boltzmann Function

The temperature dependence of the diffusion coefficient $D(T)$ can also be established by the phenomenological sigmoidal or Boltzmann function as previously reported for the temperature-induced phase transition measured by NMR spectroscopy of PNIPAm systems[29,33–36] and for bio-microgel.[9,47] The thermoresponsive polymer diffusivity in the presence of phase transition can be described by phenomenological Boltzmann function, that is

$$D(T) = \frac{A}{1+\exp\left\{\frac{(T - T_t)}{\Delta T_t}\right\}} + B \quad (9)$$

where A and B are fit parameters and the quantity ΔT_t is the width of temperature-induced phase transition. From Equation (9), in the swollen regime for $T < T_t$ we get $D_{coil} \approx A + B$, and in the plateau region of collapsed state when $T > T_t$ we can write $D_{globule} \approx B$. Finally, Equation (9) can be rewritten as a Boltzmann function

$$D(T) \approx \frac{D_{coil} - D_{globule}}{1+\exp\left\{\frac{(T - T_t)}{\Delta T_t}\right\}} + D_{globule} \quad (10)$$

where D_{coil} and $D_{globule}$ are measured diffusivity around the transition temperature or can be treated as fit parameters.

It is worth mentioning that both approaches lead to the same value of the diffusivity at phase-transition temperature, i.e., $D(T_t) = (D_{coil} + D_{globule})/2$. Furthermore, the transition width ΔT_t obtain by the temperature dependence of diffusivity using Equation (10) can be correlated to the normalized transition entropy $|\Delta S/k_B|$, and transition temperature T_t is given by Equation (8). In order to establish this relationship, we assume that the first-order derivative as a function of temperature of Equations (8) and (10) are the same at $T = T_t$. This assumption can be justified by the fact that the values of the transition temperatures obtained by the Boltzmann function and two-state model are in good agreement.[33,34] Finally, we yield

$$\Delta T_t \propto \frac{T_t}{\left(\frac{|\Delta S|}{k_B}\right)} \quad (11)$$

3.3. Temperature Dependence of Hydrodynamic Radius in the Approximation of Two-State Model

The Stokes–Einstein relation $D = k_B T/6\pi\eta R_h$ has a broad range of generality being valid for diffusion of nanoparticles and polymers. In this equation, η is the solvent dynamic viscosity and R_h is the hydrodynamic radius of the particle. Moreover, a modified Stokes–Einstein relationship that takes into account both relative solute (R_h)/solvent (R_{sol}) ratio and the shape of molecules with the major (a) and minor (b) semiaxes can be written as $D = (k_B T)/(c(R_{h,} R_{sol}) f_s(a,b)\pi\eta R_h)$.[48] It was shown that in many practical cases c and f_s factors can be balanced and, hence, the classical Stokes–Einstein relationship remains a good approximation.[48] Furthermore, this finding is supported by the measurement of diffusivity for roughened poly(styrene) particles that can be also modeled by the classical Stokes–Einstein relation.[49]

© 2018 The Authors. Published by WILEY-VCH Verlag GmbH & Co. KGaA, Weinheim

Combining $D = k_B T/6\pi\eta R_h$ relationship with Equation (8), we can write for temperature dependence of the hydrodynamic radius $R_h(T)$ in the approximation of two-state model and an average value of the solvent dynamic viscosity

$$\frac{1}{R_h(T)} \approx \frac{R_{h,coil}^{-1}}{1+\exp\left\{\frac{(T-T_t)|\Delta S|}{k_B T_t}\right\}} + \frac{R_{h,globule}^{-1}}{1+\exp\left\{-\frac{(T-T_t)|\Delta S|}{k_B T_t}\right\}} \quad (12)$$

where $R_{h,coil}$ and $R_{h,globule}$ are the average hydrodynamic radius for coil and globule in the region of phase transition, respectively. We note that the photon correlation spectroscopy gives also access to $R_h(T)$ via translational diffusivity[12,13] and the same phase-transition thermodynamic parameters can be evaluated from Equation (12) derived in the approximation of the two-state model.

4. Results and Discussion

4.1. Proton HRMAS NMR Spectroscopy

Proton HRMAS NMR spectra of Bn-PNIPAm-SH (M_n = 30 000 g mol^{-1}) and NIPAm-PNIPAm-SH (M_n = 45 000 g mol^{-1}) linear polymers were measured at concentration of c = 50 mg mL^{-1} in D_2O and are shown in **Figure 1**a and Figure 1b, respectively. For benzyl end-group functionalized polymer (Bn-PNIPAm-SH) two peaks of nonequivalent aromatic ring protons of benzyl were detected at δ_{CH2} = 7.3 ppm and δ_{CH2} = 7.4 ppm and are shown in the inset of Figure 1a. These two benzyl peaks show a significant reduction in the integral area when the phase transition is taking place. In the aliphatic spectral region, two strong peaks were detected for side chains that correspond to methyl protons of *N*-isopropyl groups (δ_{CH3} = 1.2 ppm, peak 1), and methine protons ($\delta_{CH,isopropyl}$ = 3.9 ppm, peak 2). The polymer backbone is characterized by methylene protons (δ_{CH2} = 1.6 ppm, peak 3) and methine protons ($\delta_{CH,backbone}$ = 2.1 ppm, peak 4). The protonated D_2O peak is detected at chemical shift value of δ_{HDO} = 4.8 ppm.

The methyl NMR peak 1 is most intense and narrow due to the number of protons and their fast rotation around the C_3 axis of symmetry that partially average intra- and intergoups' dipolar interactions. Hence, this peak is advantageous to be used for the measurement of stimulated spin-echo decay in diffusion NMR experiments.[1–3] Furthermore, we can note that for intermediate molecular weight of M_n = 45 000 g mol^{-1}, the ^{1}H spectrum of NIPAm-PNIPAm-SH has resonances broader compare to those of Bn-PNIPAM-SH with M_n = 30 000 g mol^{-1} (Figure 1a,b). This reduction in chain mobility is due to the hydrophilic end group, which increases the hydrodynamic drag coefficient (see the following sections).

4.2. Fractal Dimension of PNIPAm Functionalized with Hydrophobic and Hydrophilic End Groups

The diffusion decays measured by the PFGSE method of Stejskal and Tanner[37] for Bn-PNIPAm-SH and NIPAm-PNIPAm-SH linear polymers in D_2O are shown in **Figure 2**a and Figure 2b, respectively. From the *g*-dependence of detected NMR signal given by Equation (2), we can write $\ln\left(\frac{I(g)}{I(0)}\right) = -bD$, where the quantity b was varied by steps in the gradient strength. The apparent diffusivity D can be evaluated from Figure 2a, and we obtain the values of $D = 7.2 \times 10^{-11}$ m^2 s^{-1} (M_n = 5200 g mol^{-1}), and $D = 3.1 \times 10^{-11}$ m^2 s^{-1} (M_n = 30 000 g mol^{-1}) for Bn-PNIPAm-SH polymer at 20 °C. For the case of NIPAm-PNIPAm-SH, from Figure 2b we obtained at the same temperature the diffusivity $D = 8.3 \times 10^{-12}$ m^2 s^{-1} (M_n = 4000 g mol^{-1}) and $D = 1.7 \times 10^{-12}$ m^2 s^{-1} (M_n = 45 000 g mol^{-1}).

From these results we can conclude that hydrophobic (benzyl) end-group functionalized polymer has diffusivity of one order of magnitude higher compared to hydrophilic (NIPAm) end-group functionalized PNIPAm.

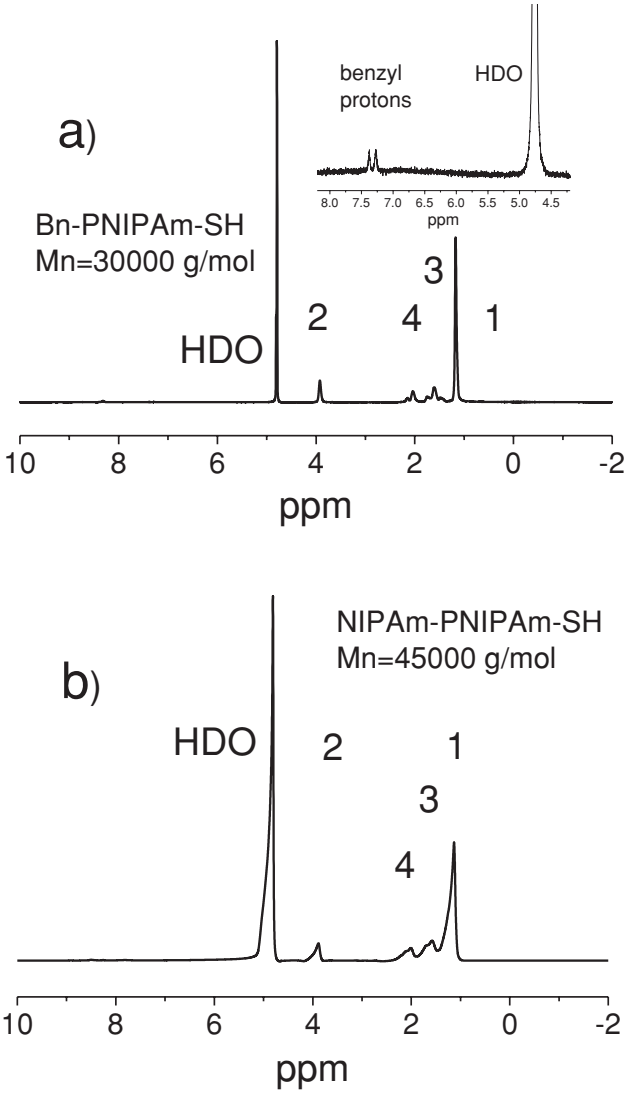

Figure 1. Proton HRMAS NMR spectra of a) Bn-PNIPAM-SH polymer with M_n = 30 000 g mol^{-1}, and b) NIPAm-PNIPAM-SH with M_n = 45 000 g mol^{-1} in deuterated aqueous solutions at 15 °C. The methyl protons of *N*-isopropyl groups correspond to peak 1 and methine protons to peak 2. Peaks 3 and 4 correspond to CH_2 and CH protons of polymer backbone.

© 2018 The Authors. Published by WILEY-VCH Verlag GmbH & Co. KGaA, Weinheim

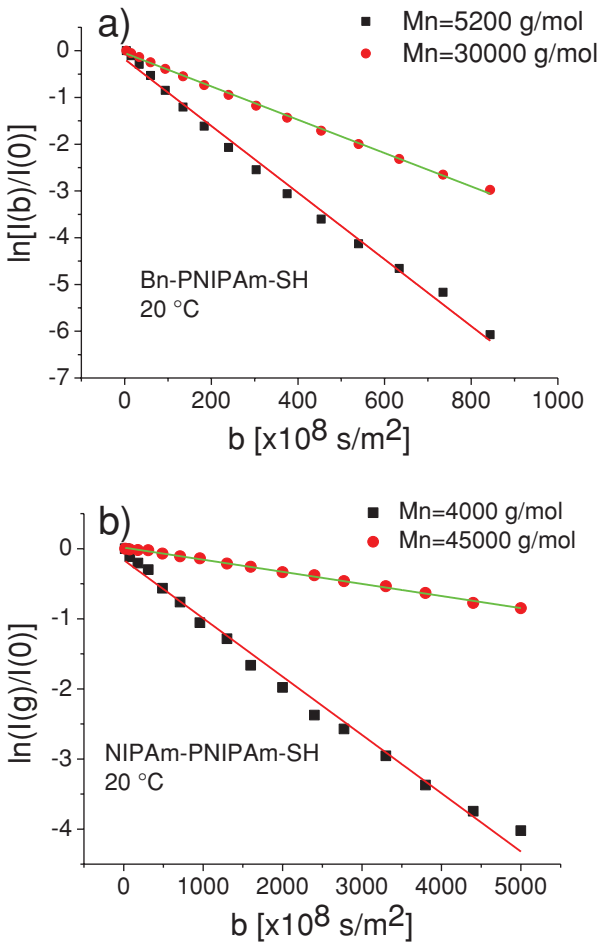

Figure 2. Diffusion decays in semilogarithmic scale for a) Bn-PNIPAm-SH and b) NIPAm-PNIPAm-SH linear polymers in D_2O with a concentration of 50 mg mL^{-1} at 20 °C. The continuous lines show linear fits using Equation (2).

The apparent diffusion coefficients of Bn-PNIPAm-SH and NIPAm-PNIPAm-SH polymers were measured for the full range of molecular weight investigated in this work and the results are shown in **Figure 3**.

The functional dependence of the radius of gyration R_g of macromolecules is related to the molecular mass M by the Flory equation[16]

$$R_g \propto M^{1/d_F} \tag{13}$$

where d_F is the fractal dimension ($1 < d_F < 3$) and $\delta = 1/d_F$ is the Flory exponent. Furthermore, for a range of molecular masses the self-diffusion coefficient D can be described by a power low. The diffusivity measurements reveal (Figure 3) for hydrophilic and hydrophobic end-group functionalization of PNIPAm a linear functional relationship in a double-logarithmic scale, that is[21]

$$D = \frac{K}{(M_n)^{1/d_F}} \tag{14}$$

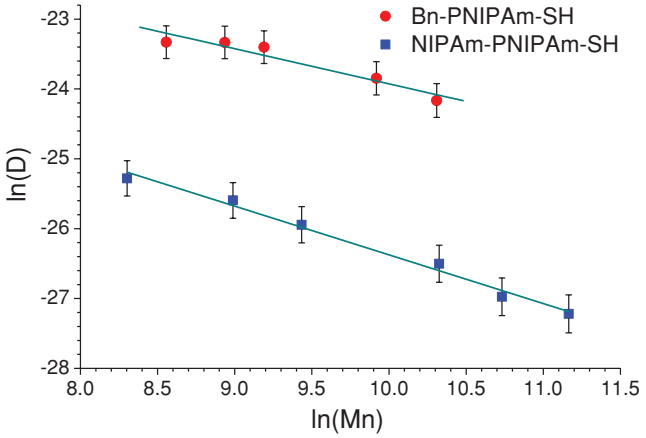

Figure 3. The dependence of diffusivity D as a function of molecular weight (M_n) in a double-logarithmic scale, for Bn-PNIPAm-SH and NIPAm-PNIPAm-SH linear polymers in D_2O with a concentration of 50 mg mL^{-1} at 20 °C. The continuous lines show the fits with linear functions.

where K is a temperature-dependent constant. From the Equation (14) and the data of Figure 3 for Bn-PNIPAm-SH and NIPAm-PNIPAm-SH linear polymers, we obtained for the fractal dimensions the values of $d_F = 2.0$ and $d_F = 1.43$, respectively. Hence, the effect of end groups upon the PNIPAm diffusivity was also revealed by the values of the fractal dimensions. Therefore, the NIPAm-PNIPAm-SH polymer coil fills less space having a larger hydrodynamic interaction compared to Bn-PNIPAm-SH coil that fills more space. Moreover, the results of Figure 3 for the investigated range of M_n show a large effect of hydrophilic and hydrophobic end groups on the values of diffusivity and, hence, a difference between polymer–solvent friction coefficients (**Table 1**). We note that the fractal dimension of $d_F = 2.0$ for linear PNIPAm was measured from polymer diffusivity at the θ temperature and it is in a very good agreement with the value reported above at 20 °C.[30] In the language of fractal objects, the fractal dimension of an ideal linear polymer is $d_F = 2.0$, while for a swollen linear chain it is $d_F = 5/3$ or $d_F \approx 1.66$.[42]

The diffusivity distributions can be obtained by inverse Laplace transformation (ILT) of the diffusion decays (Figure 2). These normalized probability distributions for Bn-PNIPAm-SH and NIPAm-PNIPAm-SH polymers, as a function of M_n, are shown in Figure S2.1 (Supporting Information). The ill-defined nature of ILT can lead to artifacts that in our case are represented by the small intensity peaks at higher values of diffusivity (Figure S2.1, Supporting Information). Figure S2.2 (Supporting Information) shows the apparent diffusivity dependence upon molecular weight on the double-logarithmic scale from the maximum of the distribution probability at 20 °C

Table 1. Drug coefficients of Bn-PNIPAm-SH and NIPAm-PNIPAm-SH linear polymers in D_2O at 20 °C.

Bn-PNIPAm-SH [g mol^{-1}]	$\xi^{a)}$ [× 10^{-11} J s m^{-2} K^{-1}]	NIPAm-PNIPAm-SH [g mol^{-1}]	$\xi^{a)}$ [× 10^{-11} J s m^{-2} K^{-1}]
5200	5.6	4000	35.7
30 000	12.9	45 000	191.4

[a)]Errors are of the order of 10%.

© 2018 The Authors. Published by WILEY-VCH Verlag GmbH & Co. KGaA, Weinheim

(intense peak in Figure S2.1 in the Supporting Information) for PNIPAm linear polymer in aqueous solutions with Bn and NIPAm end-group functionalization. The values of the fractal dimension obtained from the slop of the linear dependences are close to those obtained from the data of Figure 3. Moreover, the diffusivity distributions allow us to evaluate the dispersity in the values of D coefficients. In Figure S2.3 (Supporting Information) the diffusivity width (ΔD) versus molecular weight is shown for PNIPAm free polymer in aqueous solutions with Bn and NIPAm end-group functionalization. The diffusivity width shows an order of magnitude difference between Bn-PNIPAm-SH and NIPAm-PNIPAm-SH polymers and is related to the hydrophobic and hydrophilic characters of the end groups and fractal dimension.

The diffusivity D is based on many solvent/solute mixture upon the Einstein relationship, $D = k_B T/\xi$, where ξ is the hydrodynamic drag or frictional coefficient between polymer and solvent. This quantity is sensitive to the polymer conformations and thus will change during the temperature-induced phase transition. The frictional coefficient in the hydrodynamic limit is given by Stokes–Einstein relation, $\xi = 6\pi\eta R_h$, where η is the solvent dynamic viscosity and R_h is the hydrodynamic radius. From the data shown in Figure 3 we can evaluate the friction coefficients for end-group functionalized PNIPAm in aqueous solution as a function of molecular weight using the relation $\xi = k_B T/D$. For the extreme values of M_n investigated in this study, the friction coefficients are shown in Table 1. From these results we can conclude that in the case of hydrophilic NIPAm-like end group, the friction coefficient of the PNIPAm coil is about one order of magnitude higher compared to that of hydrophobic Bn end group with the same range of molecular weight. In the former case, the hydrogen bonding of NIPAm with the solvent molecules is responsible for the increase in the hydrodynamic drag coefficient. We note that the molecular weight of NIPAm (M_n = 113.16 g mol^{-1}) is close to that of benzyl (M_n = 92.11 g mol^{-1}) and, therefore, the difference in the polymer diffusivity is not related to the difference in M_n but to the changes in hydrodynamic interaction due to hydrophilic and hydrophobic characters of end groups.

4.3. Temperature-Induced Phase Transition of NIPAm-PNIPAm-SH and Bn-PNIPAm-SH Polymer Chains in Aqueous Solution by ^{1}H High-Resolution NMR Diffusometry

The temperature dependence of the diffusivity D of NIPAm-PNIPAm-SH linear polymer is shown in **Figure 4** for three values of the molecular weight. The same dependences are shown in **Figure 5** for Bn-PNIPAm-SH end-group functionalized polymer. In this case, the diffusivity is shifted to higher values as expected from the data shown in Figure 3. The changes in the value of the diffusion coefficients as a function of temperature reveal a phase transition from coil (swollen) state characterized by small values of D to globule (collapsed) state with higher values of D that corresponds to faster center-of-mass transport due to change in the polymer size and hydrodynamic interaction. In the swollen state, the plateau is well revealed while in the collapsed state the plateau is not clearly evidenced due to the limited range of temperature chosen to avoid convection. The increase in the value of M_n makes the plateau more visible due to the shift in the transition temperature T_t, and narrowing of the phase-transition width ΔT_t (see the following section).

It is worth mentioning that for all molecular weight and temperature investigated, leading to different overlap concentration

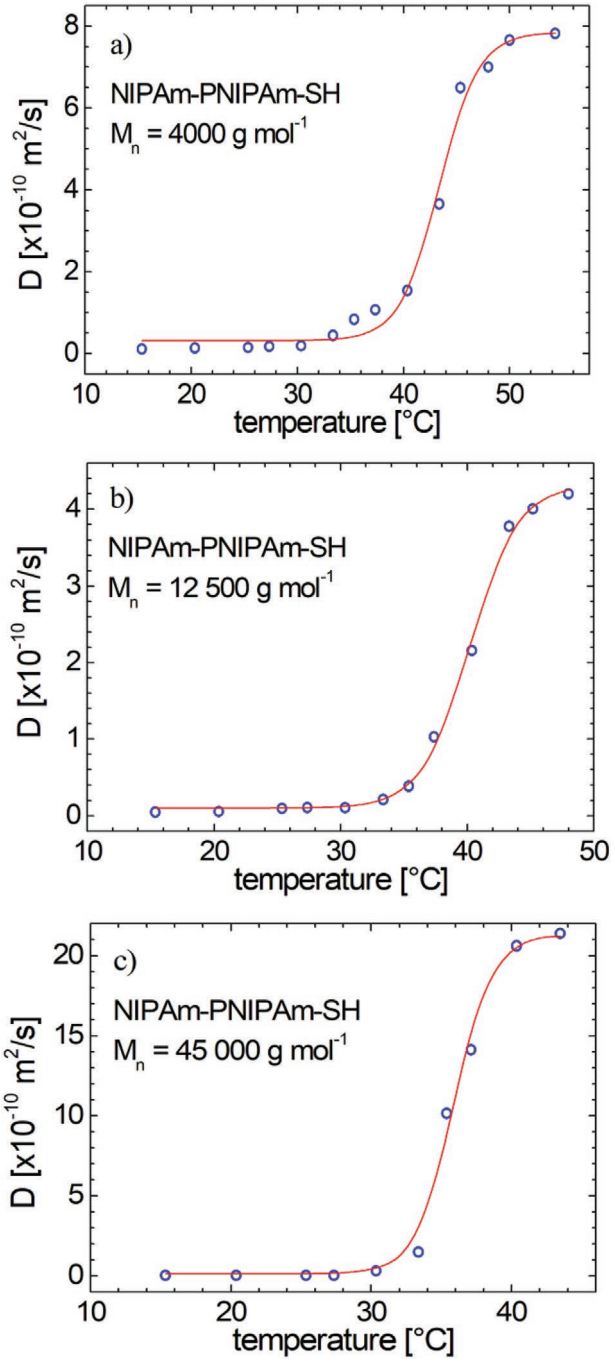

Figure 4. Temperature-induced phase transition measured by the dependence of diffusivity D as a function of temperature for NIPAm-PNIPAm-SH polymers in D_2O with a concentration of 50 mg mL^{-1}. The NIPAm-PNIPAm-SH molecular weight is a) M_n = 4000 g mol^{-1}, b) M_n = 12 500 g mol^{-1}, and c) M_n = 45 000 g mol^{-1}. The continuous lines correspond to the two-state model fits (Equation (8)).

© 2018 The Authors. Published by WILEY-VCH Verlag GmbH & Co. KGaA, Weinheim

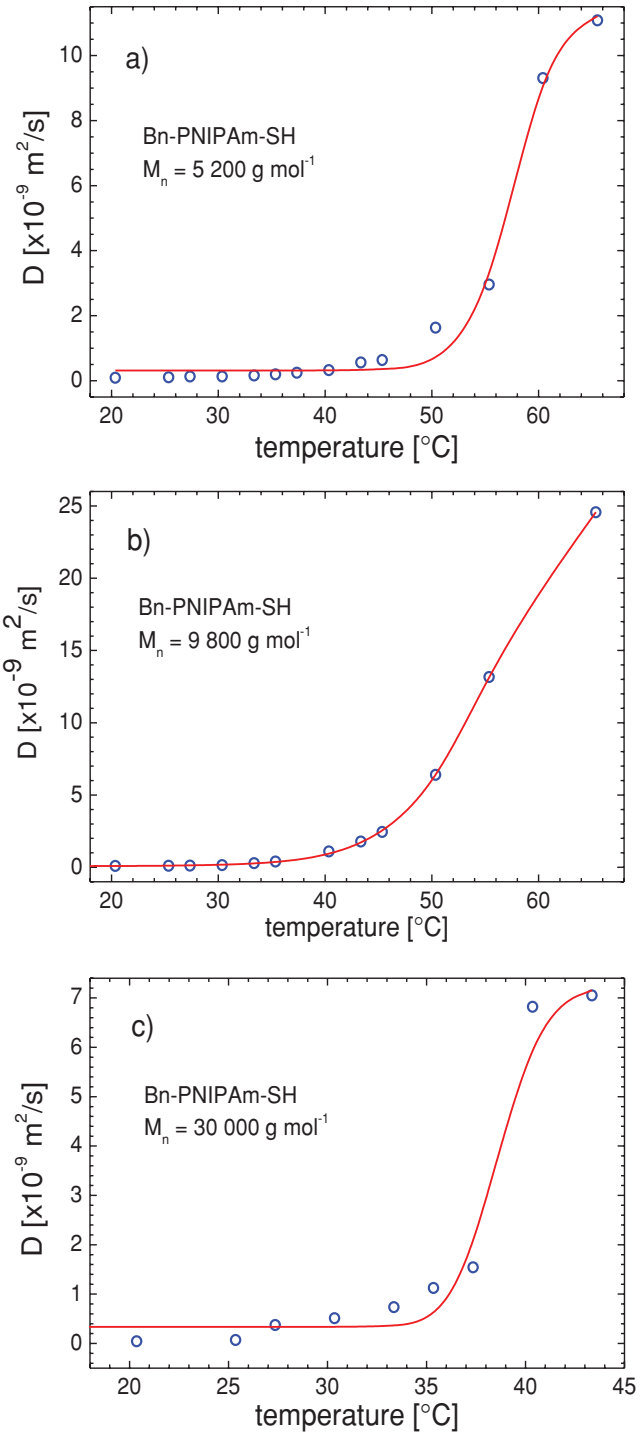

Figure 5. Temperature-induced phase transition measured by the dependence of diffusivity D as a function of temperature for Bn-PNIPAm-SH polymers in D_2O with a concentration of 50 mg mL^{-1}. The Bn-PNIPAm-SH molecular weight is a) $M_n = 5200$ g mol^{-1}, b) $M_n = 9800$ g mol^{-1}, and c) $M_n = 30\,000$ g mol^{-1}.The continuous lines show the two-state model fits (Equation (8)).

c^*, the diffusion decay curves are monoexponential showing that the presence of a heterogeneous system having globule and aggregates can be, in a good approximation, excluded. Moreover, we can evaluate the value of c^* for the particular case of PNIPAm with $M_n = 30\,000$ g mol^{-1} using the relation[42]

$$c^* = \frac{M_n}{VN_{av}} \tag{15}$$

where $V = \left(\frac{4\pi}{3}\right)R_h^3$, R_h is the hydrodynamic radius, and N_{av} is the Avogadro number. The dependence of hydrodynamic radius on molecular weight was measured for PNIPAm at 20 °C using DLS and is given by $R_h = 0.016\, M_w^{-0.54}$ (nm).[50] From Equation (15), we obtain $c^* \approx 18$ mg mL^{-1}. Hence, the PNIPAm aqueous solutions used in our investigation with $c = 50$ mg mL^{-1} are in the region of chains' overlap where the coil-to-globule transition still dominates the phase transition as was proved by self-diffusion coefficient in NMR measurements for PNIPAm with $M_w = 10^5$ g mol^{-1}.[51]

The molecular weight dependence of thermodynamic quantities T_t and $\Delta S/k_B$ (**Figure 6**a,b) was obtained by the two-state model fits (Equation (8)) of the data shown in Figures 4 and 5 for NIPAm-PNIPAm-SH (red bars) and Bn-PNIPAm-SH (black bars) polymers. The phase-transition temperature decreases with the increase in the molecular weight for both end groups (Figure 6a). The same behavior is detected from the Boltzmann function fits by Equation (10), as shown in Figures S3.1–S3.3 of the Supporting Information. This corresponds to the increase in the hydrodynamic interaction present in the diffusivity measurements with the increase in molecular weight that will lead to a decrease in T_t. This is different for the case of phase-transition temperature measured by ^{1}H HRMAS NMR spectroscopy/relaxometry that is showing opposite behavior for PNIPAm having NIPAm and Bn end groups.[34] For the case of Bn-PNIPAm-SH, the transition temperature that edit the side chain and backbone dynamics is increased with the increase in molecular weight.[34]

The trend in the changes of $|\Delta S/k_B|$ with the molecular weight is the same for NIPAm-PNIPAm-SH and Bn-PNIPAm-SH linear polymers measured by integral spectral intensity through ^{1}H HRMAS NMR spectroscopy/relaxometry[34] and NMR diffusometry (Figure 6b). The reduction in the phase-transition width ΔT_t with the increase in molecular weight for both end-group functionalization of PNIPAm measured by NMR diffusometry (Figure 6c) is in agreement with that measured before using ^{1}H HRMAS NMR spectroscopy by T_2-edited spectral intensity.[34] Furthermore, in the limit of ideal chains and not large values of molecular weight, the dependence $\Delta T_t \propto M_n^{-1/2}$ was theoretically established that it is in agreement with the dependences shown in Figure 6c for both end-group functionalization.[52]

4.4. Sensitivity of Hydrodynamic Radius Measured by NMR Diffusometry to the End Groups of PNIPAm Polymer in Aqueous Solutions

The hydrodynamic radius (R_h) for NIPAm-PNIPAm-SH and Bn-PNIPAm-SH polymer chains in the process of temperature-induced phase transition can be obtained from chains' diffusivities shown in Figures 4 and 5, respectively. The relationship between R_h and D is assumed to be given by Stokes–Einstein

© 2018 The Authors. Published by WILEY-VCH Verlag GmbH & Co. KGaA, Weinheim

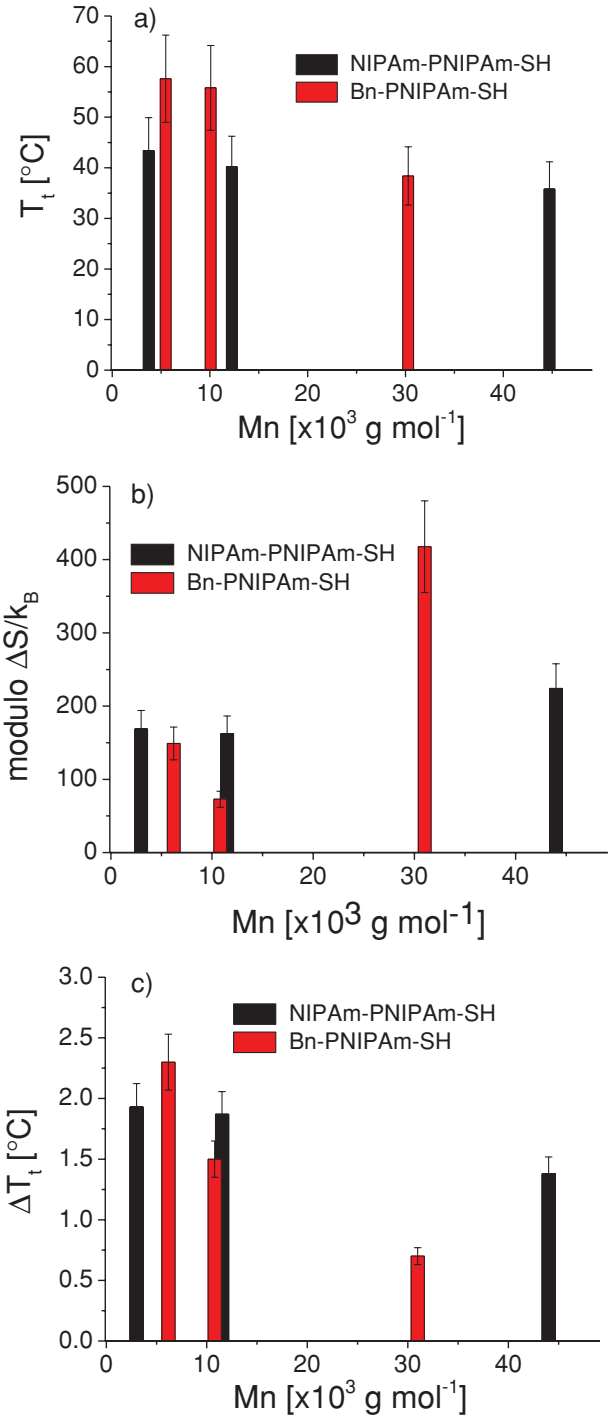

Figure 6. Thermodynamic parameters of temperature-induced phase transition given by a) transition temperature, b) change in entropy, and c) width of transition as a function of molecular weight. The width of the phase transition is obtained from the fit with the Boltzmann function (Equation (10)).

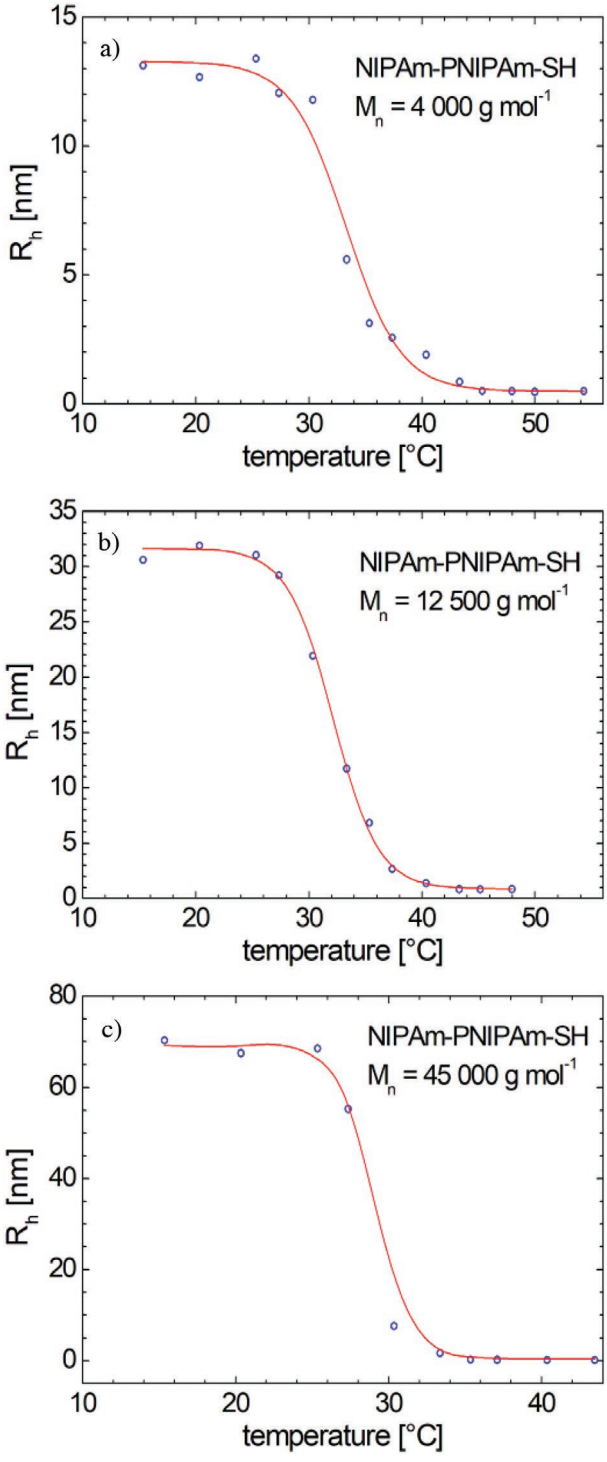

Figure 7. Temperature-induced phase transition measured by the dependence of hydrodynamic radius, R_h, as a function of temperature for NIPAm-PNIPAm-SH polymers in D_2O with a concentration of 50 mg mL^{-1}. The NIPAm-PNIPAm-SH molecular weight is a) M_n = 4000 g mol^{-1}, b) M_n = 12 500 g mol^{-1}, and c) M_n = 45 000 g mol^{-1}. The continuous lines correspond to the two-state model fits (Equation (12)).

equation and dynamic viscosity for deuterated water is taken from ref. [53]. The dependence of hydrodynamic radius as a function of temperature for PNIPAm polymers with NIPAm and Bn end groups is shown in **Figures 7** and **8**, respectively.

The above dependences show a sigmoidal shape characteristic for phase transition in the polymer overlap concentration without contributions from aggregation.

© 2018 The Authors. Published by WILEY-VCH Verlag GmbH & Co. KGaA, Weinheim

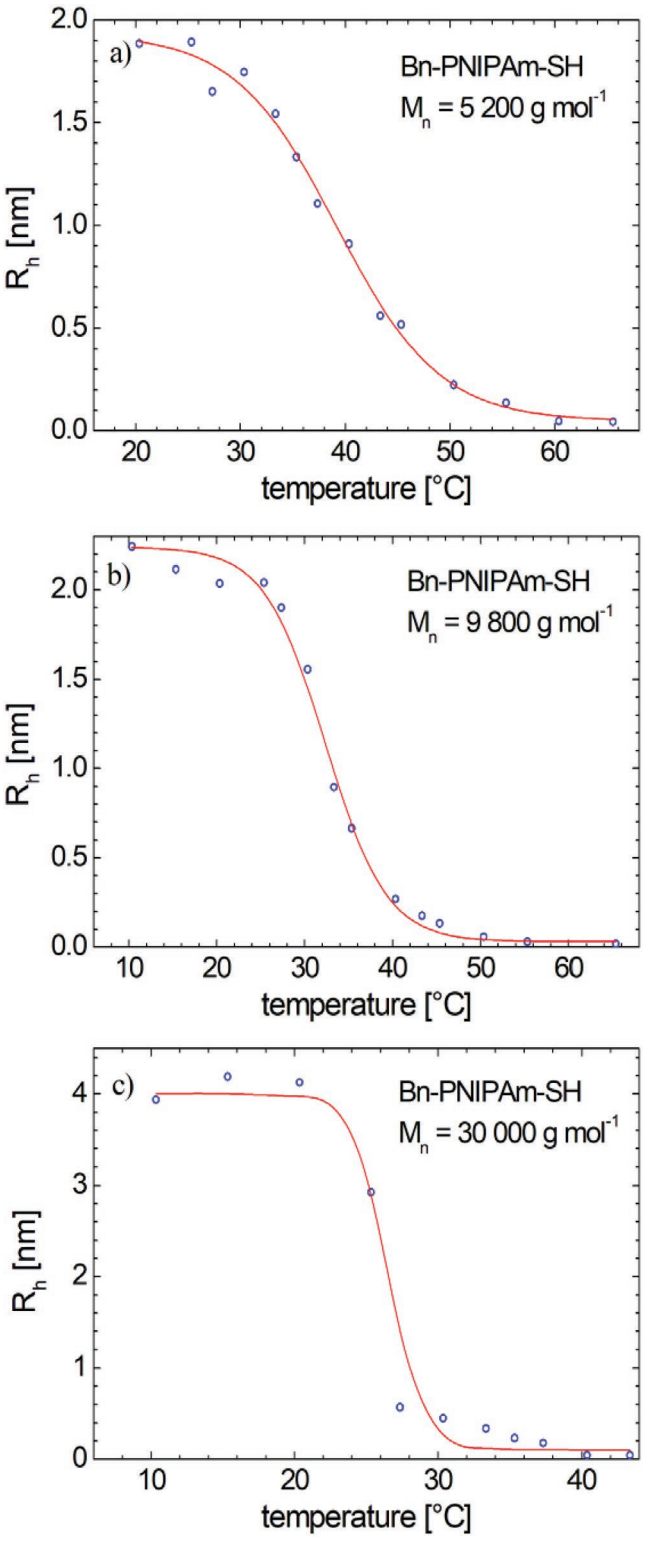

Figure 8. Temperature-induced phase transition measured by the dependence of hydrodynamic radius, R_h, as a function of temperature for Bn-PNIPAm-SH polymers in D_2O with a concentration of 50 mg mL^{-1}. The Bn-PNIPAm-SH molecular weight is a) $M_n = 5200$ g mol^{-1}, b) $M_n = 9800$ g mol^{-1}, and c) $M_n = 30\,000$ g mol^{-1}. The continuous lines show the two-state model fits (Equation (12)).

Similar $R_h(T)$ dependence describing coil-to-globule transition in the heating process was reported by Wu and Wang[38] through DLS for PNIPAm linear chains with $M_n = 1.3 \times 10^7$ g mol^{-1} in extremely dilute aqueous solution ($c = 6.7 \times 10^{-4}$ mg mL^{-1}). Furthermore, it is worth noting that the values of the hydrodynamic radius for coils show differences of one order of magnitude between NIPAm-PNIPAm-SH and Bn-PNIPAm-SH linear polymers (Figure S4.1, Supporting Information) as a consequence of differences in diffusivity (Figures 4 and 5), reflecting the effect of hydrophilic and hydrophobic end groups. As expected, R_h increases with the increase of molecular weight as shown in Figure S4.1 (Supporting Information).

The hydrodynamic radius values shown in Figure S4.1 (Supporting Information) are taken from those of Figures 7 and 8 at 20 °C. The dependence $R_h(M_n)$ is in agreement with that obtained by DLS measurement for nonfunctionalized PNIPAm with $M_n = 1.3 \times 10^7$ g mol^{-1} at 20 °C, where $R_h \approx 125$ nm was reported.[38] Furthermore, the hydrodynamic radius obtained for NMR diffusometry, as discussed in Section 3.3, are shown in the double-logarithmic scale in **Figure 9**. The linear fits lead to the following power-law relations measured at 20 °C

$$R_h^{NIPAm} = 5.35(M_n)^{0.68} \text{ nm} \quad (16)$$

and

$$R_h^{Bn} = 0.88(M_n)^{0.42} \text{ nm} \quad (17)$$

where M_n has units of kDa. Similar dependences were reported by PNIPAm linear polymer at 20 °C using static and dynamic light scattering.[54] In this case, the power-law relation was given by $R_h^{PNIPAm} \propto (M_w)^{0.57}$ nm.[54] These results show that the power-law exponents depend on the PNIPAM end groups and the polymer chains in aqueous solutions at 20 °C behave as expanded flexible coils. The coil sizes are bigger for

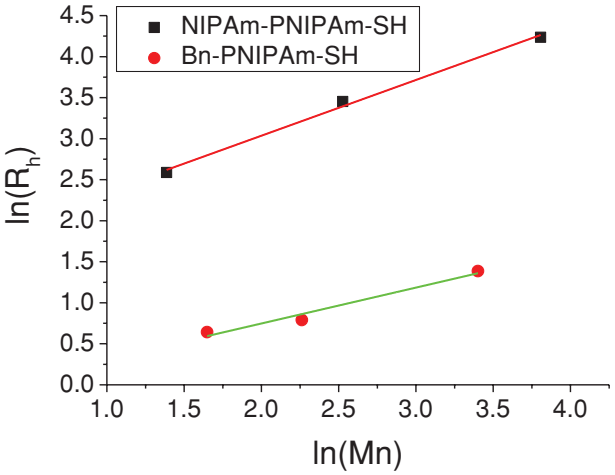

Figure 9. Hydrodynamic radius measured by NMR diffusometry for PNIPAm linear polymer in aqueous solutions with NIPAm and Bn end groups as a function of molecular weight in a double-logarithmic scale at 20 °C. The linear fits of the data are shown by continuous lines.

© 2018 The Authors. Published by WILEY-VCH Verlag GmbH & Co. KGaA, Weinheim

NIPAm-PNIPAm-SH compared to Bn-PNIPAm-SH due to the hydrophilic character of NIPAm-like end group.

5. Conclusions

The translational diffusion of stimuli-responsive polymers can be quantified in the region of phase transition using a statistical two-state model and phenomenological Boltzmann function. Both approaches describe, in a good approximation, the temperature dependence of diffusivity measured by pulsed-field gradient stimulate-echo NMR diffusometry in the regime where phase transition dominates the aggregation process.

The thermodynamic parameters of the temperature-induced phase transition such as transition temperature, transition entropy, and width of transition can be evaluated from these two approaches and are functions upon the molecular weight and the end-group functionalization. The dependence of the thermodynamic parameters upon M_n measured by ^{1}H high-resolution NMR diffusometry shows the same trend for both hydrophilic (NIPAm-like) and hydrophobic (Bn) end-group functionalization of PNIPAm. The polymer chain diffusivity is smaller for hydrophilic end groups compared to hydrophobic ones due to the presence of hydrogen bonding with water molecules. For the hydrophobic end groups, the solvation shell leads to a smaller hydrodynamic drag coefficient. In the presence of end-group functionalization, the difference in the polymer diffusivity becomes smaller with the increase of polymer molecular weight that starts to be dominated by the interactions of polymer segments. The fractal dimension measurements show that the NIPAm-PNIPAm-SH coil fills less space compared to Bn-PNIPAm-SH coil that fills more space, which explains the differences in diffusivity. NMR diffusometry allows us to measure the hydrodynamic radius of polymers and to establish the dependences of power-law relations upon end groups' interactions with water molecules.

In general, the thermodynamic parameters of the phase transitions for thermosensitive polymer solutions are reflected in a different manner into measurements sensitive to overall polymer translation or rotation. The former case corresponds to diffusivity measurements and the latter case to NMR methods based on the side chain and segmental dynamics edited by integral intensity of the HRMAS spectra.[33,34] Hence, the characterization by diffusometry and NMR spectroscopy of temperature-induced phase transition in responsive polymers is complementary. The diffusivity measurements by stimulated-echo normalization are not sensitive to the T_2 relaxation rates and, therefore, give an independent access to the parameters of temperature-induced transition and discriminate between translation and rotation polymer motions. Moreover, we note that Equation (5) is generally describing the diffusivity of stimuli-responsive polymer chains, brushes, and microgels, independent of the method used for diffusion coefficient measurement.

The results discussed in this work will allow us to obtained more insights into the aggregation process of stimuli-sensitive polymer brushes onto nanoparticles like AuNRs, by its dependence on particle concentration and temperature, pH, ionic strength, or near-infrared laser irradiation.

Supporting Information

Supporting Information is available from the Wiley Online Library or from the author.

Acknowledgements

M.M. gratefully acknowledges the support of an Advanced Grant from the European Research Council (ERC), Jellyclock 695716. The funding from DFG-SFB 985 was also gratefully acknowledged. This work was performed in part at the Center for Chemical Polymer Technology CPT, which was supported by the EU and the federal state of North Rhine-Westphalia (Grant No. EFRE 30 00883 02). The authors thank Dr. Helmut Keul and Dr. Rostislav Vinokur for useful discussions.

Conflict of Interest

The authors declare no conflict of interest.

Keywords

diffusion, end-group functionalization, NMR, poly(*N*-isopropylacrylamide), temperature-induced phase transition

Received: November 30, 2017
Revised: February 22, 2018
Published online: April 15, 2018

[1] P. T. Callaghan, *Translational Dynamics and Magnetic Resonance*, Oxford University Press, New York, NY **2011**.
[2] R. Kimmich, *NMR Tomography, Diffusometry, Relaxometry*, Springer-Verlag, Berlin **1997**.
[3] W. S. Price, *NMR Studies of Translational Motion*, Cambridge University Press, Cambridge **2009**.
[4] J. Kärger, D. M. Ruthven, *New J. Chem.* **2016**, *40*, 4027.
[5] D. E. Demco, C. Filipoi, X. Zhu, R. Fechete, M. Möller, *Macromol. Chem. Phys.* **2013**, *214*, 1345.
[6] Y. E. Shapiro, *Prog. Polym. Sci.* **2011**, *36*, 1184.
[7] T. Ohkubo, A. Ohira, Y. Iwadate, *J. Phys. Chem. Lett.* **2012**, *3*, 1030.
[8] A. Rollet, J. Simonin, R. Turq, A. Vandais, J. Noel, C. Malveau, D. Canet, *J. Phys. Chem. B* **2001**, *105*, 4503.
[9] S. Singh, D. E. Demco, K. Rahimi, R. Fechete, J. C. Rodriguez-Cabello, M. Möller, *Soft Matter* **2016**, *12*, 6240.
[10] A. Dolgopolov, K. N. Grafskaia, D. V. Anokhin, D. E. Demco, X. Zhu, D. A. Ivanov, M. Möller, *Phys. Chem. Chem. Phys.* **2017**, *19*, 7714.
[11] C. Nicholson, *Rep. Prog. Phys.* **2001**, *64*, 815.
[12] R. Pecora, *J. Chem. Phys.* **1968**, *49*, 1036.
[13] K. Schmitz, *An Introduction in Dynamic Light Scattering by Macromolecules*, Academic Press, Boston, MA **1990**.
[14] M. Eigen, E. L. Elson, *Proc. Natl. Acad. Sci. USA* **1994**, *91*, 5740.
[15] T. Wohland, R. Friedrich, R. Hovius, H. Vogel, *Biochemistry* **1999**, *38*, 8671.
[16] P. Flory, *Principles of Polymer Chemistry*, Cornell University Press, Ithaca, NY **1953**.
[17] P. de Gennes, *Scaling Concepts in Polymer Physics*, Cornell University Press, New York, NY **1953**.
[18] S. Viel, D. Capitani, L. Mannina, A. Segre, *Biomacromolecules* **2003**, *4*, 1843.
[19] C. A. Crutchfield, D. J. Harris, *J. Magn. Reson.* **2007**, *185*, 179.
[20] K. Chari, B. Antalek, J. Minter, *Phys. Rev. Lett.* **1995**, *74*, 3624.

© 2018 The Authors. Published by WILEY-VCH Verlag GmbH & Co. KGaA, Weinheim

[21] S. Augé, P.-O. Schmit, A. C. Crutchfield, M. T. Islam, D. J. Harris, E. Durand, M. Clemancy, A.-A. Quoineaud, J.-M. Lancelin, Y. Prigent, F. Taulelle, M.-A. Delsue, *J. Phys. Chem. B* **2009**, *113*, 1914.
[22] M. Doi, S. Edwards, *The Theory of Polymer Dynamics*, Oxford University Press, Oxford **1986**.
[23] P. K. Jain, X. Huang, I. H. El-Sayed, M. A. El-Sayed, *Acc. Chem. Res.* **2008**, *41*, 1578.
[24] B. P. Timko, M. Arruebo, S. A. Shankarapps, J. B. McAlvin, O. S. Okankwa, B. Mizrahi, C. F. Stefanescu, L. Gomez, J. Zhu, J. Santamaria, R. Langer, D. S. Kohane, *Proc. Natl. Acad. Sci. USA* **2014**, *28*, 1349.
[25] M. Mitsuishi, M. Koishikawa, Y. H. Tanaka, E. Sato, T. Mikayama, J. Matsui, T. Miyashita, *Langmuir* **2007**, *23*, 7472.
[26] M. Kurg, S. Jaber, T. Hellweg, T. Mulvaney, *Langmuir* **2011**, *27*, 820.
[27] A. Mourran, H. Zhang, R. Vinokur, M. Möller, *Adv. Mater.* **2017**, *29*, 1604825.
[28] J. Rubio Retama, B. Frick, T. Seydek, M. Stamm, A. Fernnandez Barbero, E. López Cabaros, *Macromolecules* **2008**, *41*, 4739.
[29] M. Rusu, S. Wohlrab, D. Kuckling, H. Möhwald, M. Schönhoff, *Macromolecules* **2006**, *39*, 7358.
[30] R. Plummer, D. J. T. Hill, A. K. Whittaker, *Macromolecules* **2006**, *39*, 8379.
[31] B. Sierra-Martin, Y. Choi, M. S. Romero-Cano, T. Cosgrove, B. Vincent, A. Fernández-Barbero, *Macromolecules* **2005**, *38*, 10782.
[32] P. V. Yushmanov, I. Furó, I. Iliopoulos, *Macromol. Chem. Phys.* **2006**, *207*, 1972.
[33] S. Schweizerhof, D. E. Demco, A. Mourran, H. Keul, R. Fechete, M. Möller, *Macromol. Chem. Phys.* **2017**, *218*, 16004951.
[34] S. Schweizerhof, D. E. Demco, A. Mourran, H. Keul, R. Fechete, M. Möller, *Macromol. Rapid Commun.* **2017**, *38*, 1700362.
[35] J. Spevacek, J. Dybal, L. Starovoytova, A. Zhigunov, *Soft Matter* **2012**, *8*, 6110.
[36] C. M. Burba, S. M. Carter, K. J. Meyer, C. V. Rice, *J. Phys. Chem. B* **2008**, *112*, 10399.
[37] E. O. Stejskal, J. E. Tanner, *J. Chem. Phys.* **1965**, *42*, 288.
[38] C. Wu, X. Wang, *Phys. Rev. Lett.* **1998**, *80*, 4092.
[39] W. McPhee, K. C. Tam, R. Pelton, *J. Colloid Interface Sci.* **1993**, *156*, 24.
[40] K. Chan, R. Pelton, J. Zhang, *Langmuir* **1999**, *15*, 4018.
[41] V. O. Aseyev, H. Tenhu, F. H. Winnik, *Adv. Polym. Sci.* **2006**, *196*, 1.
[42] M. Rubinstein, R. H. Colby, *Polymer Physics*, Oxford University Press, Oxford, NY **2003**.
[43] G. Karlström, *J. Phys. Chem.* **1985**, *89*, 4962.
[44] A. Matsuyama, F. Tanaka, *Phys. Rev. Lett.* **1990**, *65*, 341.
[45] S. Bekiranov, R. Bruinsma, P. Pincus, *Phys. Rev. E* **1997**, *55*, 577.
[46] V. A. Baulin, A. Halperin, *Macromolecules* **2002**, *35*, 6432.
[47] S. Singh, D. E. Demco, K. Rahimi, R. Fechete, J. C. Rodriguez-Cabello, M. Möller, *Macromol. Rapid Commun.* **2016**, *37*, 181.
[48] A. Macchioni, G. Ciancaleoni, C. Zaccaccia, D. Zaccaccia, *Chem. Soc. Rev.* **2008**, *37*, 479.
[49] B. W. Longbottom, B. Samuncuoglu, F. J. Punter, S. Longbottom, A. F. Bon, *Soft Matter* **2017**, *13*, 4285.
[50] K. Kubota, S. Fujishige, I. Ando, *Polym. J.* **1990**, *22*, 15.
[51] A. Larsson, D. Kuckling, M. Schönhoff, *Colloids Surf., A* **2001**, *190*, 185.
[52] A. Yu. Grosberg, A. R. Khokhlov, *Statistical Physics of Macromolecules*, AIP Press, New York, NY **1994**.
[53] R. C. Hardy, R. L. Cottington, *J. Chem. Phys.* **1949**, *17*, 509.
[54] K. Kubota, K. Hamano, N. Kuwahara, S. Fujishige, I. Ando, *Polym. J.* **1990**, *22*, 1051.

© 2018 The Authors. Published by WILEY-VCH Verlag GmbH & Co. KGaA, Weinheim